2016. Journal of Arachnology 44:153–164

The hemolymph vascular system in A*raneus diadematus* with special focus on intraspecific variability in artery systems

Jens Runge and **Christian S. Wirkner**: Universität Rostock, Allgemeine & Spezielle Zoologie, Institut für Biowissenschaften, Universitätsplatz 2, 18055 Rostock, Germany. E-Mail: jens.runge@uni-rostock.de

Abstract. The European garden spider, *Araneus diadematus* Clerck, 1757, is one of the most common spiders in central Europe. However, despite its abundance, comparatively little is known about its internal anatomy. We therefore conducted an examination of the hemolymph vascular system (HVS) of *A. diadematus*, as part of a comparative survey on the circulatory system in spiders. The HVS of *A. diadematus* was investigated using micro-computed-tomography and serial sectioning and visualized using 3D-reconstruction software. In order to examine the HVS for intraspecific variability, over 30 specimens were studied in detail. The HVS of *A. diadematus* consists of a tubular heart, which is situated along the dorsal midline of the opisthosoma. Anteriorly, the heart gives rise to the anterior aorta and posteriorly to the posterior aorta. Three pairs of cardiac arteries originate from the dorso-lateral section of the heart and the branching pattern of these arteries in *A. diadematus* is visualized and described here for the first time. The anterior aorta runs through the pedicel into the prosoma where it branches to supply the muscles and organs with hemolymph. The central nervous system in particular is supplied by a large number of arteries, which show some interesting branching patterns, e.g., a unilateral origin of the transganglionic arteries in the subesophageal ganglion, and the supply of the lower lip by the first of these transganglionic arteries. Furthermore, there are a number of arteries in the HVS with unilateral (asymmetrical) origins. Some cases of intraspecific variability are demonstrated, e.g., for the arteries of the upper and the lower lip. The data presented here are discussed in reference to information on the HVS in Araneae available in existing literature.

Keywords: 3D imaging, micro-CT, right-left asymmetry

The earliest descriptions of the hemolymph vascular system (HVS) in Araneae can be traced back to the beginning of the 19th century (e.g., Cuvier 1810, pp. 257–263; Treviranus 1812) and, in the decades which followed, there was a marked increase in the interest this organ system generated (Brandt 1840; Grube 1842; Blanchard 1849; Schimkewitsch 1884). Although there has been a lot of interest in the opisthosomal part of this organ system, the prosomal HVS has received less attention (Claparède 1863; Causard 1896; Petrunkevitch 1911; Willem 1917; Crome 1952). However, the particularly detailed results presented by Schneider (1892) and Causard (1896) have had a significant influence on our perception of the vascular system in spiders.

In essence, the circulatory system of Araneae, as in other arthropods, can be divided into two parts: a) the HVS, consisting of the heart and arteries and, b) the hemolymph lacunar system, comprising sinuses and lacunae (Wirkner 2009; Wirkner et al. 2013). The hemolymph is distributed throughout the body by the pumping heart via artery systems. At the ends of the arteries, the hemolymph leaves the HVS and enters the hemolymph lacunar system. Within this latter system, the hemolymph is channeled to the book lungs and from there the oxygenated hemolymph is channeled – via sinuses – to the pericardial sinus. Here the hemolymph reenters the heart lumen via ostia, slit-like openings in the wall of the heart (see e.g., Wirkner & Huckstorf 2013).

In the context of a comprehensive survey on the circulatory system in Araneae, we present here the results of a detailed study on the HVS in the species *Araneus diadematus* Clerck, 1757 using up-to-date morphological analysis and visualization methods. Morphological descriptions are usually generalized by species and, after a series of intermediate steps, it is possible to attain an evolutionary analysis of organ systems (Richter & Wirkner 2014). However the problem of intraspecific variability has often been neglected in morphological studies. In Crustacea, it is known that different arterial patterns can occur within one species (Keiler et al. 2013) and even within genetically homogenous populations as in *Procambarus fallax* (Hagen, 1870) f. *virginalis* (Vogt et al. 2009). To be able to effectively generalize morphological results with respect to one species, a large data set must be obtained. We studied 33 specimens of *A. diadematus* using micro-computed-tomography (micro-CT) and 3D-reconstructions to provide a detailed morphological description of the HVS, with special focus on intraspecific variability of arterial patterns.

METHODS

Animals.—The specimens of *A. diadematus* were collected in the urban area of Rostock (Mecklenburg-Western Pomerania, Germany) in October 2010, and between August and November 2011. Around 100 adult and penultimate females and seven adult males were obtained. The body length of the females ranged from 8–18 mm; in the males the range was between 5 and 6 mm. Only males were used for semi-thin sectioning (see below). Additionally, one specimen of *Araneus quadratus* Clerck, 1757 was studied. This sample was collected in September 2010 on the island of Hiddensee (Mecklenburg-Western Pomerania, Germany).

The spider taxonomy employed follows 'The World Spider Catalog' (2015).

Ninety-two of the female specimens were treated using the injection method – as detailed in the following section. To verify the quality of the injection, injected specimens were checked using micro-CT. Ultimately, 33 specimens (injected and uninjected) were scanned and used for further 3D investigation. Table 1 shows the different procedures used to

Table 1.—The applied treatments and methods for the considered 33 specimens. Ad: *Araneus diadematus*; Aq: *Araneus quadratus*; CPD: critical point dryer; KOH: potassium hydroxide.

Specimen-ID	Method	Sex	Injection (resin)	Tissue treatment	Contrasting treatment
Ad01, Ad03 Ad12, Ad13 Ad14, Ad15 Ad16, Ad17	micro-CT	f	PU4ii	KOH (maceration)	Lugol's solution
Ad04, Ad05 Ad07, Ad10 Ad11	micro-CT	f	-	Dubosq-Brasil	alcoholic Iodine-solution
Ad06	micro-CT	m	-	Dubosq-Brasil	alcoholic Iodine-solution
Ad08	micro-CT	f (penultimate)	-	Dubosq-Brasil	alcoholic Iodine-solution
Ad30	semi-thin sections	m	-	Dubosq-Brasil	azure II and methylene blue
Ad39, Ad40	micro-CT	m	-	Dubosq-Brasil	alcoholic Iodine-solution
Ad41, Ad43 Ad44, Ad45 Ad46, Ad47 Ad48	micro-CT	f	PU4ii	Bouin	PU4ii mixed with 1% iodine enriched Butanon; Lugol's solution
Ad69	micro-CT	f	PU4ii	Bouin	Lugol's solution; alcoholic Iodine-solution
Ad72, Ad86	micro-CT	f	PU4ii	Bouin	Lugol's solution
Ad92, Ad94	micro-CT	f	Mercox II	Bouin	alcoholic Iodine-solution; CPD
Ad95	micro-CT	f	Mercox II	Bouin	alcoholic Iodine-solution
Ad105	micro-CT	f	Mercox II	Dubosq-Brasil	alcoholic Iodine-solution
Aq01	micro-CT	f	PU4ii	Bouin	alcoholic Iodine-solution

treat each of the 33 specimens. When referring to a specific specimen, the assigned Specimen-ID (see Table 1) is given, e.g., in figure legends.

Injection of resin.—To prepare casts of HVS, we followed the methods as described by Wirkner & Richter (2004). Spiders were anesthetized with a lethal dose of chloroform and then injected with resin. We used the casting resin Mercox II (Ladd Research Industries, USA) or the polyurethane Pu4ii (vasQtec, Univ. of Zurich, Switzerland). Just before being injected, the resin was mixed with a hardener (Pu4ii) or a catalyst (Mercox II) and put into a 5 ml syringe (Braun Injekt®, Luer Solo) that was locked onto a medical infusion set, 0.4 × 20 mm in size (servoprax, Wing Flo®, Luer Lock). The injection setup was finely adjusted using a mechanical micromanipulator. The legs of the spiders were removed during the injection procedure so the resin could leave the body. To allow the resins to polymerize and temper, the specimens were left for several minutes after the injection. Mercox II-injected and uninjected specimens were fixed in Duboscq-Brasil fixative (10 parts: saturated picric acid dissolved in 96% ethanol, 4 parts: 37% formaldehyde, 1 part: glacial acetic acid), while Pu4ii-injected specimens were fixed in Bouin's fluid (15 parts: saturated aqueous picric acid, 5 parts: 40% formaldehyde, 1 part: acetic acid). To ensure enhanced contrast, preparations later used for micro-CT were stored for at least 12 hours in alcoholic iodine-solution or in Lugol's solution (aqueous iodine potassium iodide solution) (Metscher 2009). The prosomata and the opisthosomata of the animals were separated at the pedicel to aid the fixing and contrasting process. This method was exclusively applied to female specimens.

Specimens with a good injection result were critical-point-dried (EMITECH K850, UK) to further ameliorate contrast.

Micro-computed-tomography (micro-CT).—X-ray scans were performed using the Phoenix Nanotom® (Phoenix|X-ray, GE Sensing & Inspection Technologies) high-resolution micro-CT system in high-resolution mode (target: molybdenum, mode: 0–1; performance: ca. 3–6 W; number of images: 1440; detector-timing: 1500–5000 ms; voxel size: ca. 4–8 μm). The surrounding medium of the specimens during the scan was distilled water, ethanol, or air depending on the initial fixing and contrasting procedure.

Semi-thin section series.—Histological semi-thin section series were carried out for male specimens. For this purpose, the prosoma was removed from the opisthosoma and fixed in Bouin's fixative. It was then dehydrated in ethanol and, after an intermediate step of epoxypropane, embedded in araldite epoxy resin under vacuum. Serial semi-thin sections (1 μm) were made with a Leica Ultracut UCT microtome using a diamond knife. The sections were stained with a mixture of 1% azure II and 1% methylene blue in aqueous 1% borax solution for approximately 5–25 s at 80–90°C.

3D reconstruction.—The image stacks produced using micro-CT were loaded into the software Imaris 7.0.0 by Bitplane to create all 3D-reconstructions. A scene was created in the program module 'Surpass'. To visualize whole data sets, the volume rendering function was chosen. The contours of the studied morphological structures were marked with a polygon on virtual cross sections.

Images/Illustration.—All figure plates were arranged using the Corel Graphics Suite X3. Images were embedded into Corel Draw X3 files and edited in Corel PhotoPaint X3 using general imaging enhancement tools (contrast, brightness).

The PDF version of the current study is equipped with interactive 3D-content. Three-dimensional objects resulting from the aforementioned 3D-reconstruction process were converted using Adobe 3D-Reviewer (version: 9.0.0.107). To activate the 3D-content, click on the desired image and use the mouse buttons to navigate.

RESULTS

The following section predominantly comprises a description of the HVS in *A. diadematus* and, as the heart constitutes the central organ of the whole system, it is a logical starting point. The terminology employed follows the ontology of arthropod circulatory systems (OArCS; Wirkner unpubl. data). In accordance with this ontology, only single un-

branched arteries are termed 'artery system', such as 'first cardiac artery system'. Complete vascular trees, i.e., arteries and all their branches are termed 'artery system', for example 'first cardiac artery system'. An artery system is named after the stem artery, to which all its branches can be traced back.

The morphological descriptions that follow are divided into two parts. The first part comprises the description of stable morphological patterns, which were observed in all specimens. The second part, 'Variability', considers morphological patterns that were found to differ between specimens. The numerical ratios by which certain patterns were observed are given in this context.

HVS of the opisthosoma.—*The heart:* The heart of *A. diadematus* lies in the dorso-medial region of the opisthosoma. It runs in an anterior direction from the third pair of the dorso-ventral muscles to the posterior end of the pedicel. In the anterior part of the opisthosoma, the heart bends (in a slight s-shape) ventrally toward the pedicel but not directly adjacent to the anterior cuticle (the opisthosoma overhangs the pedicel here) (Figs. 1A & C, 2A).

At its posterior end, the heart merges into the posterior aorta. The posterior aorta runs towards the spinnerets where it splits at their distal end. The posterior aorta system does not show any further ramifications (Fig. 1B, D, E). Anteriorly, the heart is extended by the anterior aorta, which supplies the whole prosoma.

Three pairs of ostia are located on the lateral side of the heart and three pairs of cardiac arteries originate on the ventro-lateral side of the heart (Fig. 2). The first pair of ostia is situated on a dilatation of the myocard which is situated dorsally to the bending of the heart toward the pedicel. These ostia are oriented in a dorso-ventral direction. The second and the third pairs of ostia are located in the dorso-lateral region of the heart. They lie dorsally to the origins of the first and second cardiac artery systems, respectively. The second pair of ostia is located in the heart region between the most anterior pair of dorsal muscles and the first pair of dorso-ventral muscles. The third pair of ostia lies between the first and second pair of dorso-ventral muscles. The third pair of cardiac artery systems arises laterally to the origin of the posterior aorta system at the posterior end of the heart.

Cardiac artery systems: Three pairs of cardiac artery systems originate from the heart. The first and second pairs of cardiac artery systems originate ventro-laterally to the second and third pair of ostia, respectively (Fig. 2A). The third pair of cardiac artery systems originates at the posterior end of the heart, laterally to the origin of the posterior aorta system. All three pairs of cardiac artery systems run to the periphery of the opisthosoma (Fig. 1B, interactive 3D content).

The first pair of cardiac artery systems mainly supplies the antero-lateral part of the opisthosoma (Fig. 1B, C). The second system supplies the central region of the opisthosoma (Fig. 2B, C) and it includes a prominent stem artery, the second cardiac artery, which runs to the ventral muscle cord. Numerous smaller arteries with anterior or posterior orientation originate from the second cardiac artery, which also divides into two equally sized arteries dorsally to the ventral muscle cord.

The third pair of cardiac artery systems supplies the postero-lateral part of the opisthosoma (Fig. 1B, C).

Variability: There is one artery of the third cardiac artery system (Fig. 1D, E; ca3*) that splits off medially and runs postero-ventrally to the stercoral pocket. Every specimen displayed a unilateral occurrence of this artery, however in six specimens the origin was observed to be at the right third cardiac artery, and at the left cardiac artery in a single specimen.

It should be noted that here we describe variable patterns of major arteries. Variability in smaller arteries is not in the scope of this study and should be a topic of further investigations (see also Discussion).

Ligaments of the heart: The heart is suspended by ten pairs of dorsal ligaments, nine pairs of lateral ligaments and three pairs of ventral ligaments (Fig. 2). The dorsal ligaments are attached to the dorsal midline of the heart at regular intervals. They are attached almost rectangular to the heart from where they run to the dorsal cuticle of the opisthosoma. Only the tenth dorsal ligaments run at a more oblique angle: in this case the dorsal attachment points are in a posterior direction. Each pair of dorsal ligaments comprises two single ligaments, which lie close to each other at the attachment sites at the heart and diverge dorsally.

The lateral ligaments originate at the dorso-lateral side of the heart and run laterally to the cuticle. The third, seventh and ninth lateral ligaments attach at the apodemes of the dorsal muscle (dm), the second dorso-ventral muscle (dvm2) and third dorso-ventral muscle (dvm3), respectively (Fig. 2A, B).

The ventral ligaments originate at the ventro-lateral sides of the heart. The first pair of ligaments runs postero-ventrally between the dorsal muscles. The second pair of ventral ligaments originates medially to the origins of the second cardiac artery system and runs ventrally between the ovaries. The third pair of ventral ligaments originates medially to the third cardiac artery system and runs ventrally along the ventral side of the stercoral pocket (Fig. 2A).

HVS of the prosoma.—*Anterior aorta system:* The anterior aorta system supplies the whole prosoma (Fig. 3). The anterior aorta (Fig. 3B; aa) emanates anteriorly from the heart, which runs dorsally through the pedicel. On reaching the stomach, the anterior aorta splits into two aortic arches which flank the stomach laterally (Fig. 3B; interactive 3D content; aoa). Shortly after this first split, the paired third dorsal prosomal artery system (Fig. 3A, B; dpa3) splits off dorsally and supplies the dorsal musculature of the posterior prosoma by numerous ramifications. Anterior to the third dorsal prosomal artery system, the peribuccal artery system (Fig. 3B; pba) originates. This artery system supplies the dorsal dilatator musculature of the sucking stomach.

Posterior to the supraesophageal ganglion, the aortic arches bend ventrally and run along the dorsal surface of the subesophageal ganglion. In this region, the aortic arches give rise to four pairs of leg arteries (l1, l2, l3, l4), an unpaired first median transganglionic artery (mtga1) and an unpaired supraneural artery (sa). The pedipalpal arteries (pa) originate from the first leg arteries in close proximity to where they split off the aortic arches (Fig. 3A; interactive 3D content).

Cheliceral artery systems: The cheliceral artery systems (Fig. 3A, B; cha) originate in the dorsal bend of the aortic arches.

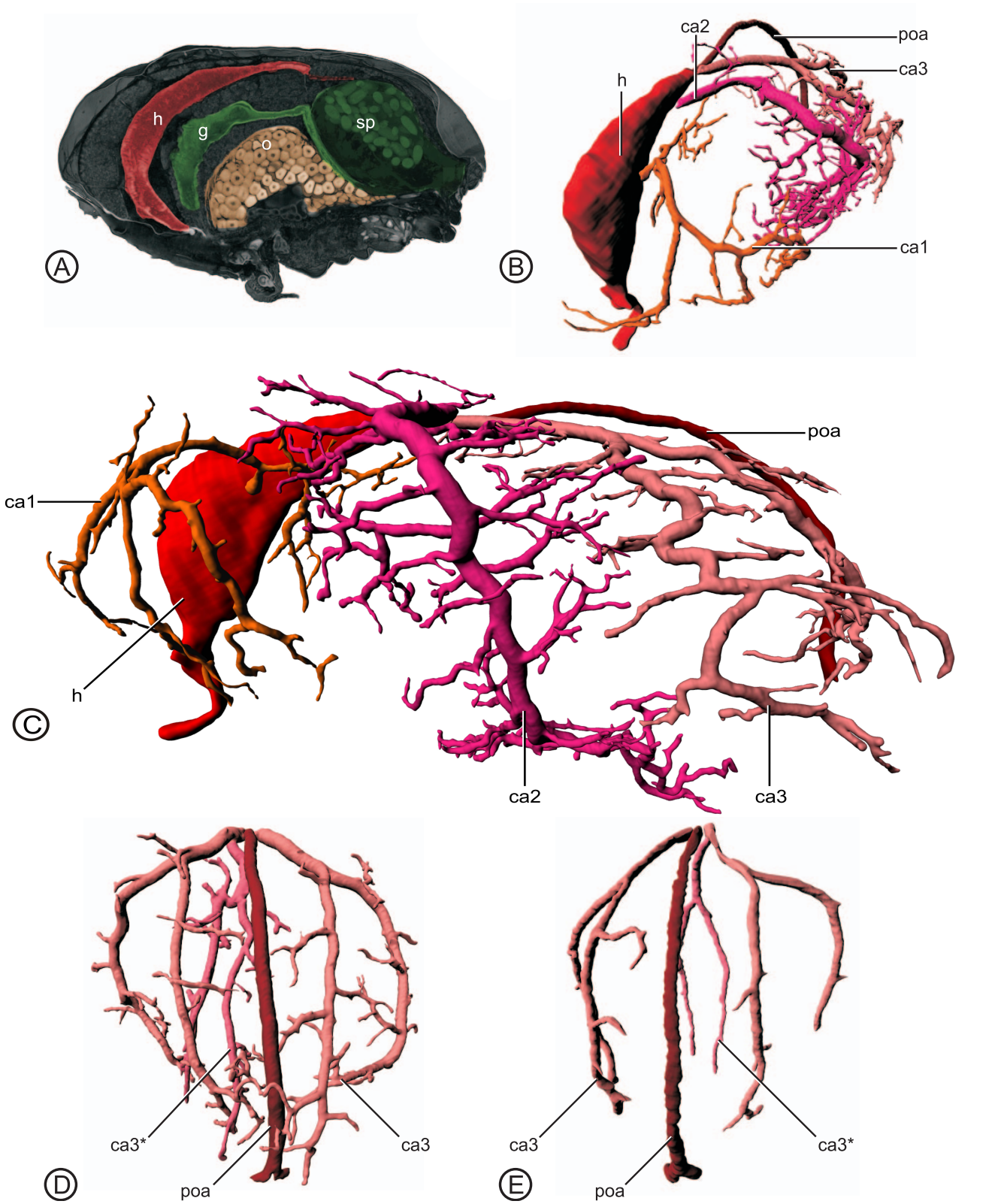

Figure 1.—Hemolymph vascular system in the opisthosoma of *A. diadematus*. PDF version contains interactive 3D content. To activate click on Fig. 1C in Adobe Reader. Rotate object with mouse and see further functionalities in content menu. **A.** Volume rendering of the opisthosoma showing the position of the heart (red), digestive organs (green) and ovaries (beige). Virtual section through the median sagittal plane; lateral view. Specimen-ID: Ad11. **B, C.** Surface rendering showing the hemolymph vascular system in the opisthosoma. Right-sided cardiac artery systems are hidden but are included in the digital 3D content of Fig. 1C. Specimen-ID: Ad01. **B.** Antero-lateral view. **C.** Lateral view. **D, E.** Surface rendering of the posterior aorta system and third cardiac artery systems showing the varying origin of the asymmetric artery (pink);

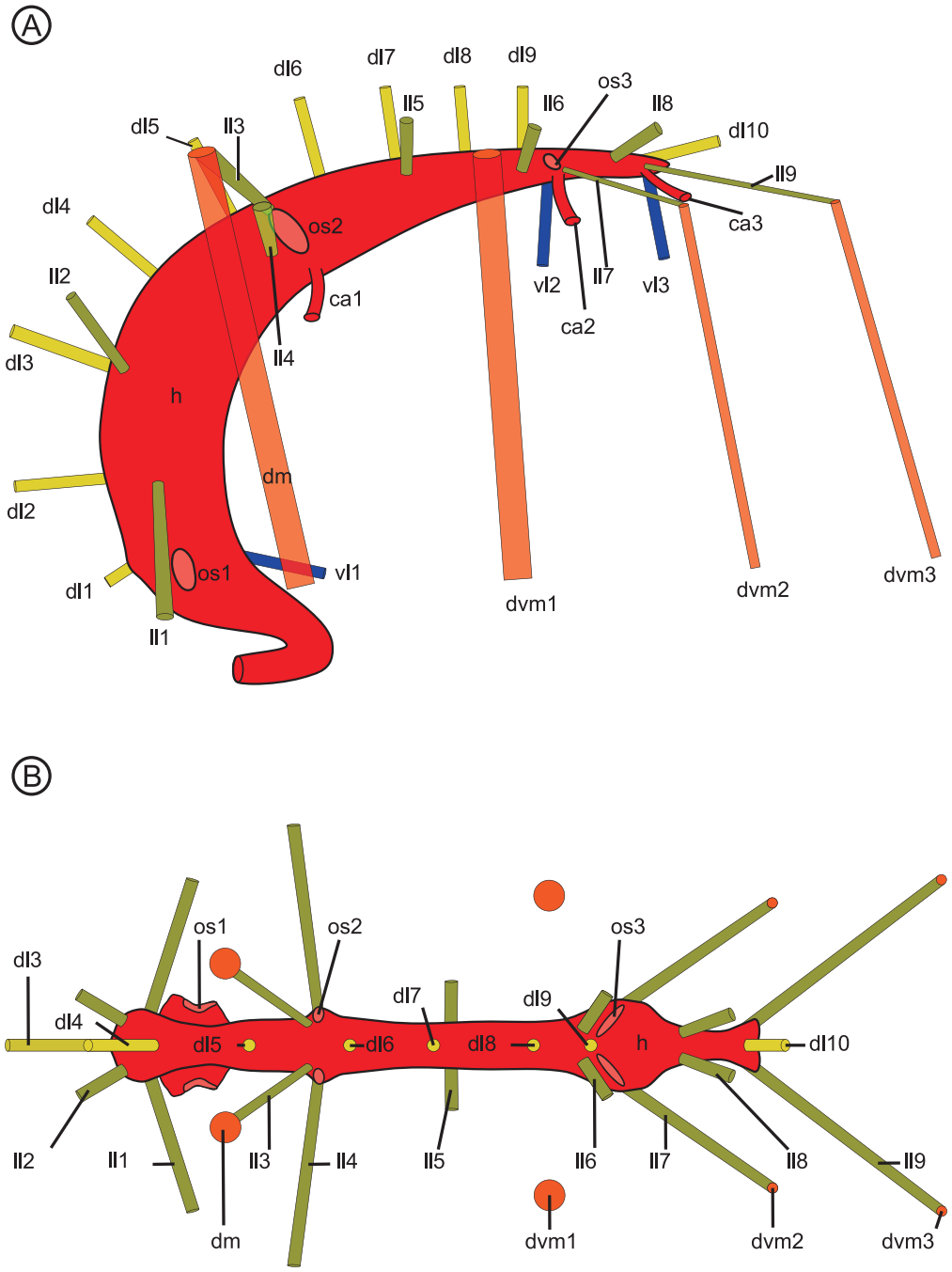

Figure 2.—Schematic drawings of the heart, cardiac artery systems and ligaments in spatial relation to the opisthosomal dorsal and dorso-ventral muscles in *A. diadematus*. **A.** Lateral view. **B.** Dorsal view. ca1–3: first–third cardiac artery; dl1–10: first–tenth dorsal ligament; dm: dorsal muscle; dvm1–3: first–third dorso-ventral muscle; h: heart; ll1–9: first–ninth lateral ligament; os1–3: first–third ostium; vl1–3: first–third ventral ligament.

They supply the anterior region of the prosoma and the chelicerae. Before the cheliceral arteries enter the chelicerae, some major artery systems originate. The optic artery systems (Fig. 3A, B; oa) run dorsally and bend anteriorly towards the eyes. After reaching the median eyes, the optic arteries arch laterally towards the lateral eyes (Fig. 3B, C). The optic artery systems also supply the venom glands (Fig. 3A–C; vg) and the dorsal musculature of the anterior prosoma.

←
posterior view. **D.** Asymmetric artery originating from the left third cardiac artery system (ca3*). Specimen-ID: Ad03. **E.** Asymmetric artery originating from the right third cardiac artery system (ca3*). Specimen-ID: Ad45. ca1–3: first–third cardiac artery system; g: gut; h: heart; o: ovary; poa: posterior aorta system; sp: stercoral pocket.

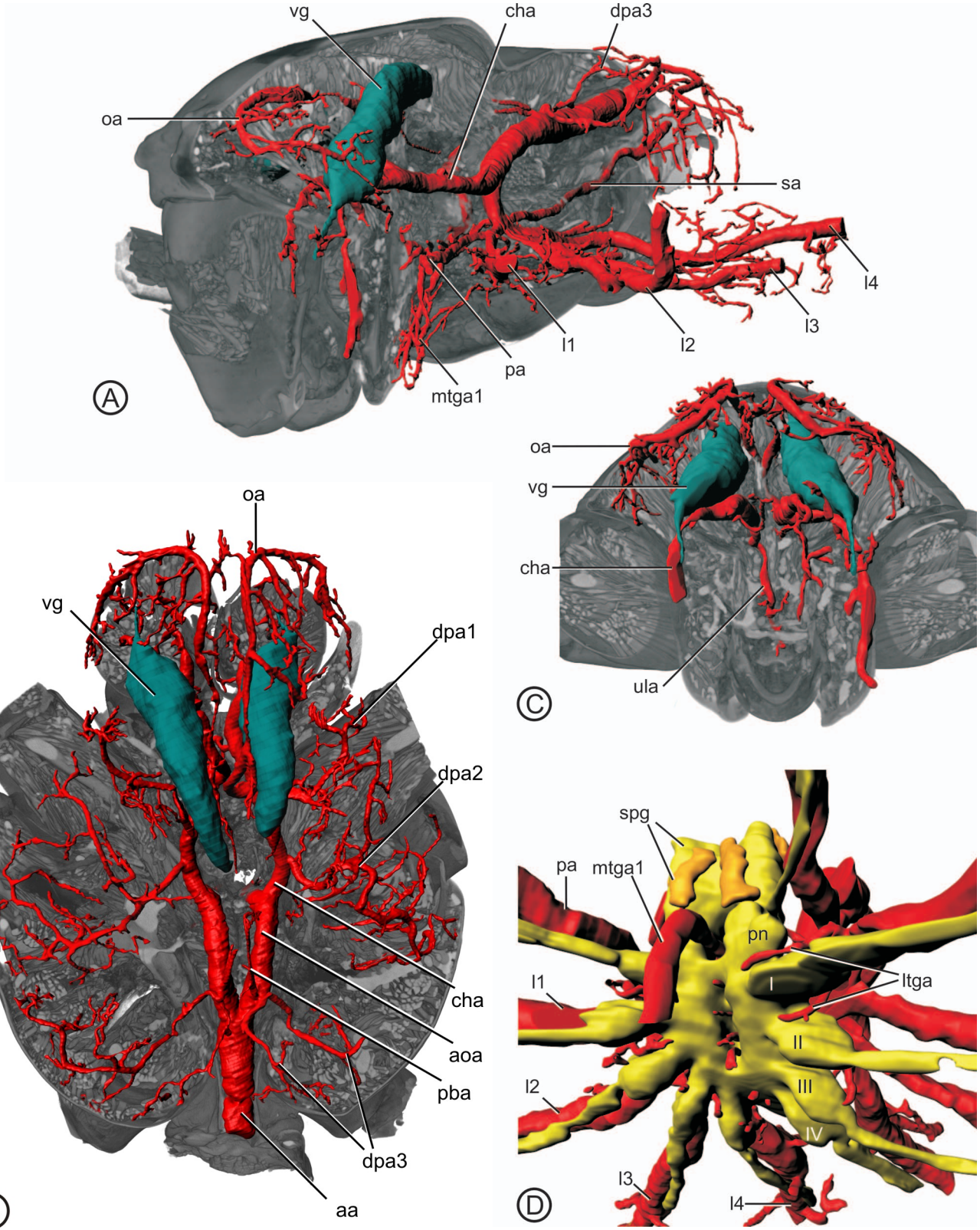

Figure 3.—Hemolymph vascular system in the prosoma of *A. diadematus*. PDF version contains interactive 3D content. To activate click on Fig. 3B in Adobe Reader. Rotate object with mouse and see further functionalities in content menu. **A–C.** Surface rendering of the hemolymph vascular system (red) and the venom glands (cyan) in the prosoma (volume rendering). Specimen-ID: Ad69. **A.** Antero-lateral view; dorsal branching artery systems of the cheliceral artery system are hidden but are included into the digital 3D content of Fig. 3B. **B.** Dorsal view. **C.** Anterior view. **D.** Surface rendering of the hemolymph vascular system and the central nervous system; ventro-lateral view. Specimen-ID: Aq01.

The dorsal musculature of the medial portion of the prosoma is supplied by two paired arteries: the first (dpa1) and the second dorsal prosomal artery systems (dpa2). They originate from the proximal part of the cheliceral arteries (Fig. 3A, B).

The unpaired upper lip artery system (Fig. 3C; ula) originates from one (see 'Variability' below) cheliceral artery. The upper lip artery runs postero-ventrally before it bends ventrally into the upper lip.

Variability: We observed that the origin of the upper lip artery system was not consistent. In five specimens, the upper lip artery originated in the right cheliceral artery and, in another five specimens, it originated in the left cheliceral artery.

Leg artery systems and pedipalpal artery systems: The aortic arches split radially into the four leg artery systems, running dorsally to the subesophageal ganglion (Fig. 3A, D; l1, l2, l3, l4); the first leg artery systems run in an antero-lateral direction, the second leg artery systems in a lateral direction, the third leg artery systems in a postero-lateral direction and the fourth leg artery systems in a posterior direction. There are just a few arteries that branch off in the proximal regions of the leg arteries. Exceptions to this are the pedipalpal artery systems at the first leg arteries, and the lateral transganglionic arteries at each leg artery. The majority of small ramifications at the leg arteries are located inside the leg. These secondary arteries supply the leg musculature. All leg arteries run dorsally along their respective leg nerves (Fig. 3D).

The pedipalpal arteries (Fig. 3A; pa) originate in the proximal region of the first leg arteries and pass the supraesophageal ganglion laterally, nearly at the same level as the esophagus penetrates the supraesophageal ganglion (Fig. 3D). The pedipalpal arteries are located dorsally on the pedipalpal neuropils. The pedipalpal arteries divide and these arteries supply the large coxal podomere and the distal pedipalpus, respectively (Fig. 3A; interactive 3D content).

Supraneural artery system: The unpaired supraneural artery system originates at the medial side of one aortic arch, or in the transient area to the most proximal region of one fourth-leg artery. The supraneural artery runs posteriorly along the median line of the body resting on the dorsal side of the opisthosomal nerve. The supraneural artery represents the origin of the posterior group of the median transganglionic arteries (mtga) (further details on mtga are provided below in "Supply of the central nervous system"). This artery traverses the pedicel ventrally to the opisthosomal nerve, however, it seem that it does not enter the main part of the opisthosoma, as the injected resin stopped abruptly at the posterior end of the pedicel.

Variability: The origin of the supraneural artery system can either be found on the left (in six specimens) or the right (in three specimens of *A. diadematus* and in the specimen of *A. quadratus*) aortic arch. No correlation was found between the originating sides of the first median transganglionic artery and the supraneural artery; all four possible combinations were present in *Araneus* (Fig. 4).

Supply of the central nervous system (prosomal ganglion): The supraesophageal ganglion is supplied by two pairs of ventral branching arteries originating at the ventro-medial side of the cheliceral arteries (Fig. 5; vb1, vb2). They run postero-ventrally into the supraesophageal ganglion and end there.

The subesophageal ganglion is supplied by two groups of arteries: the median transganglionic arteries (mtga) and the lateral transganglionic arteries (ltga).

The unpaired median transganglionic arteries penetrate the subesophageal ganglion along the midline in a regular pattern. They run to the ventral side of the subesophageal ganglion where they end openly (Fig. 3D; mtga). The number of observed, i.e., injected median transganglionic arteries varied from 5 to 12 (in 4 specimens of *A. diadematus* and the specimen of *A. quadratus*; for a more detailed analysis, see 'Discussion'). Despite the variety in the number of median transganglionic arteries, our study detected differing sites of origin: the arteries branch off the first median transganglionic artery, off one aortic arch or off the supraneural artery.

The first median transganglionic artery (Fig. 3A; interactive 3D content; mtga1) originates from the medial side of one aortic arch dorsally to the subesophageal ganglion. This artery penetrates the prosomal ganglion and runs ventrally along the esophagus (Fig. 3D). Posterior to the pharynx, the first median transganglionic artery bends ventrally and enters the lower lip with numerous ramifications. A varying number of median transganglionic arteries originate from the first median transganglionic artery (for further details see 'Variability' below).

Variability: The origin of the first median transganglionic artery system is either on the left (in four specimens of *A. diadematus* and in the specimen of *A. quadratus*) or the right aortic arch (in seven specimens).

A more detailed account of the median transganglionic arteries of two specimens is now presented, because a more generalized description was not possible:

Specimen Ad86 (with twelve detected mtga): The first median transganglionic artery originates from the right aortic arch. The second to seventh anterior median transganglionic arteries originate from the larger first median transganglionic artery. The subsequent five posterior median transganglionic arteries originate from the supraneural artery. The supraneural artery originates from the left aortic arch (Fig. 5A).

Specimen Aq01 (with eleven detected mtga): The first median transganglionic artery originates from the left aortic arch. The second to third anterior median transganglionic arteries originate from the larger first median transganglionic artery. The subsequent two median transganglionic arteries originate from the right aortic arch. The subsequent six median transganglionic arteries originate from the supraneural artery (Fig. 5B). The supraneural artery originates from the right aortic arch.

The six pairs of lateral transganglionic arteries (ltga) arise at the leg arteries and pedipalpal arteries. They run ventrally

←

I–IV: first–fourth walking leg neuropil; aa: anterior aorta system; aoa: aortic arch; cha: cheliceral artery system; dpa1–3: first–third dorsal branching artery system; pba: peribuccal artery system; l1–4: first–fourth leg artery system; ltga: lateral transganglionic arteries; mtga1: first median transganglionic artery system; oa: optical artery system; pa: pedipalpal artery system; vg: venom glands; pn: pedipalpal neuropil; sa: supraneural artery system; spg: supraesophageal ganglion; ula: upper lip artery system.

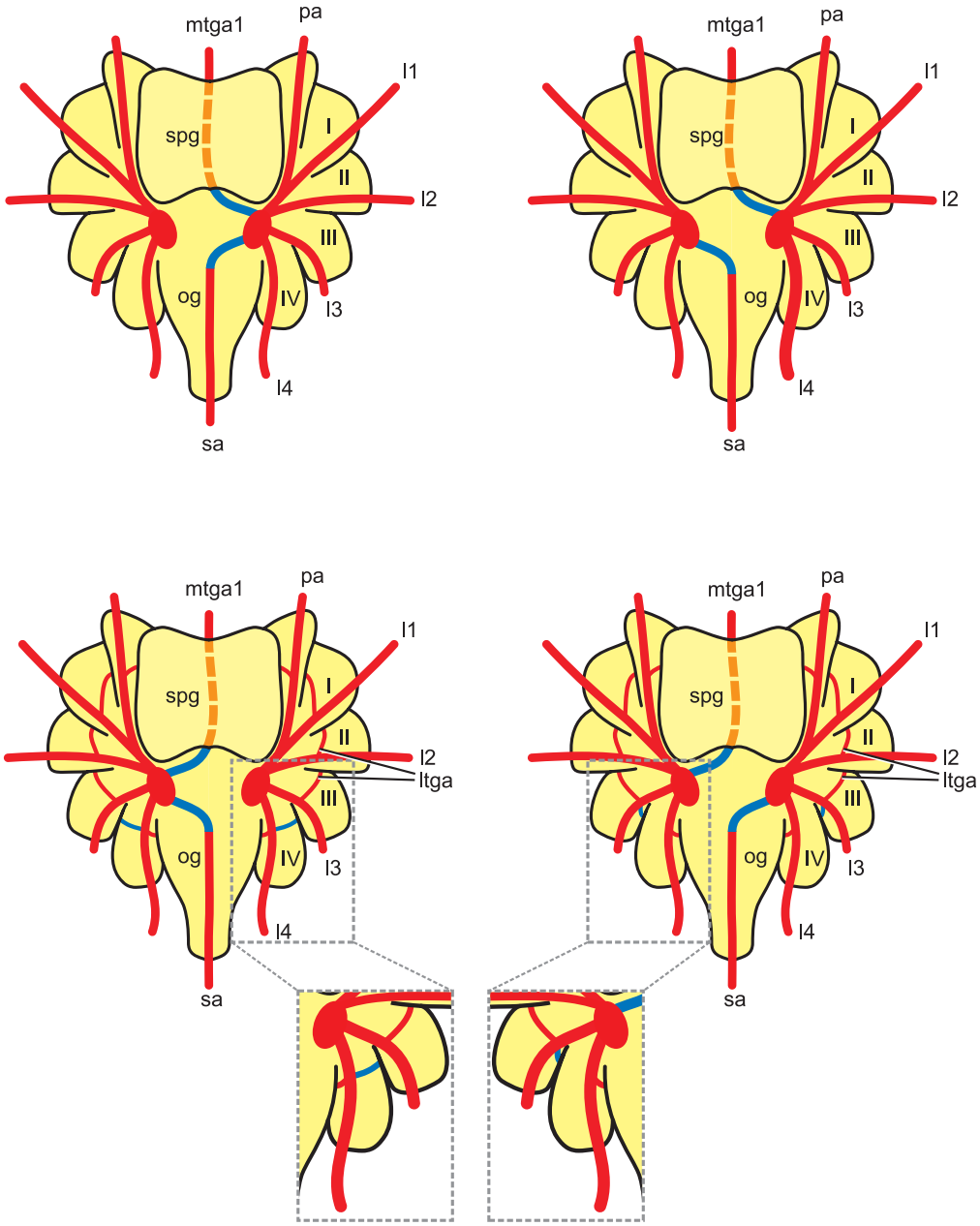

Figure 4.—Schematic drawings illustrating intraspecific variability in the origin (blue) of artery systems (red) in the region of the central nervous system (yellow); dorsal view. The four schemes show all possible combinations of origins of the first median transganglionic artery and the supraneural artery system. The lower row of schemes also shows the different origins of the lateral transganglionic arteries. I–IV: first–fourth walking leg neuropil; l1–4: first–fourth walking leg artery; ltga: lateral transganglionic arteries; mtga1: first median transganglionic artery; og: opisthosomal ganglion; pa: pedipalpal artery; sa: supraneural artery; spg: supraesophageal ganglion.

between the lateral processes of the subesophageal ganglion (Fig. 3D; ltga). At the ventral side of the subesophageal ganglion, all lateral transganglionic arteries bend medially and end openly. The lateral transganglionic arteries arising from the pedipalpal and first to third leg arteries always have their origin at the anterior side. Thus the first lateral transganglionic arteries (originating from the pedipalpal arteries) lie anterior to the pedipalpal neuropil. The subsequent lateral transganglionic arteries originating from the first to third walking leg arteries conform to the same pattern. The last two pairs of lateral transganglionic arteries are an exception to this pattern, surrounding the fourth leg neuropil anteriorly and posteriorly. So the most posterior lateral transganglionic arteries, between the fourth leg neuropil and opisthosomal ganglion always originate at the posterior side of the fourth leg artery (Fig. 4).

Variability: The lateral transganglionic arteries running between the third and fourth leg neuropils can either originate at the posterior side of the third leg artery (in one specimen) or at the anterior side of the fourth leg artery (in six specimens and one specimen of *A. quadratus*), but always symmetrically in each specimen (Fig. 4).

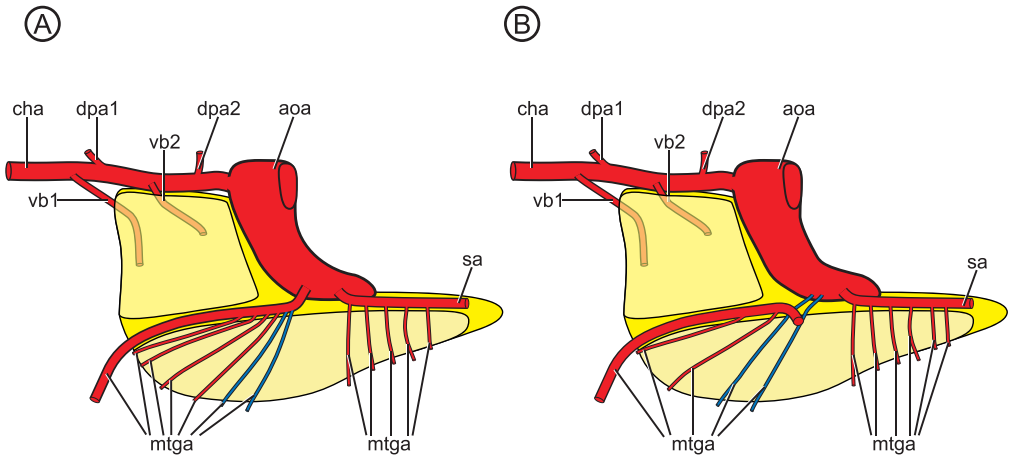

Figure 5.—Schematic drawings illustrating intraspecific variability (blue) concerning the median transganglionic arteries in the hemolymph vascular system (red) in the region of the central nervous system (yellow); lateral view. Exemplified on the specimens **A.** Ad86 and **B.** Aq01. aoa: right aortic arch (partially); cha: cheliceral artery system (partially); dpa1–2: first–second dorsal branching artery; mtga: median transganglionic arteries; sa: supraneural artery system; vb1–2: first–second ventral branching artery.

There are further arteries supplying the region between the subesophageal ganglion and the sternum, which are not in direct contact with the central nervous mass. These arteries stem from all four leg arteries before they enter the legs, and from the first median transganglionic artery before it enters the lower lip (not shown).

DISCUSSION

Comparative morphology of the HVS in the prosoma.—Only a handful of studies describing arteries in *Araneus diadematus* currently exist, and there is indeed only one study (Schneider 1892) that describes prosomal artery systems. Generally within Araneae, the course of the anterior aorta and its two aortic arches is corresponding (Schneider 1892; Causard 1896; Gerhardt & Kaestner 1938; Crome 1952; Huckstorf et al. 2013, 2015). However, in the following section, differences in the branching patterns of prosomal vascular systems in Araneae are discussed.

Our study indicates that the dorsal prosoma in *A. diadematus* is supplied by five paired artery systems: the optic artery system (oa), three dorsal prosomal artery systems (dpa1–3) and the peribuccal artery system (pba). This indicates two more dorsal artery systems than previously described by Schneider (1892). As Schneider (1892) correctly identified, the anteriormost off-branching artery system (her "nv", fig. 28) supplies the venom glands. However, we found differences with respect to the orientation of this artery system and the region it supplies. A large artery of both artery systems bends anteriorly by flanking main parts of the venom gland (see Fig. 3B), and not posteriorly as described by Schneider (1892). Indeed, only a small part of the venom glands is supplied by a separate, posteriorly-running artery. Furthermore, this artery system supplies the whole anterior region on each side of the prosoma from the median eyes to the lateral eyes and is therefore termed the optic artery system here. No such description of this course of the optic artery system in *A. diadematus* existed until now. However, similar optic artery systems have been described for other species (*Tegenaria* sp.: Schneider 1892; *Agelena labyrinthica* (Clerck, 1757): Causard 1896).

Apart from the optic artery system, two further artery systems are described by Schneider (1892); a dorsal prosomal artery system posterior to the optic artery system (which cannot definitely be equated to the first or the second dorsal prosomal artery system described in the present study), and an artery system supplying the dorsal dilatator muscles of the stomach, which can be matched to the herein described peribuccal artery system. Our study therefore identifies two additional dorsal prosomal artery systems in *A. diadematus*, and describes them here for the first time; one originates from the cheliceral artery (Fig. 3B; 3D content; dpa1 or dpa2), and the other – the third dorsal prosomal artery system (Fig. 3A, B, 3D content; dpa3 – originates from the anterior aorta after its first division. A comparable number of dorsal prosomal arteries with comparable supplied regions were described in *Cupiennius salei* (Keyserling, 1877) (Huckstorf et al. 2013). In *C. salei*, two paired dorsal prosomal arteries (their "dorsal branches of the cheliceral artery") originate from the cheliceral artery, as in *A. diadematus*. The third dorsal prosomal artery system in *C. salei* (their "dorsal artery of the anterior aorta") exhibits notable differences as it is unpaired, and originates posteriorly to the first ramification of the anterior aorta.

Furthermore, we can demonstrate that the origin of the upper lip artery system lies anterior to that of the optic artery system on the cheliceral artery (6 specimens). These results throw new light on Schneider's (1892) study, which previously described the origin of the upper lip artery system to be posterior to the optic artery system.

Arterial supply of the prosomal ganglion: Two pairs of arteries, which have not been identified before in *A. diadematus*, supply the supraesophageal ganglion. In *C. salei*, however, three pairs of arteries originating from the cheliceral artery have been shown to supply this region of the brain (Huckstorf et al. 2013). It remains unclear however, whether the number of supraesophageal arteries contains phylogenetic information, or whether it correlates with size of the supraesophageal ganglion.

With regards to the subesophageal ganglion, the lateral transganglionic arteries have been described for *A. labyrinthica* by Causard (1896), *C. salei* by Huckstorf et al. (2013) and for *Kukulcania hibernalis* (Hentz, 1842), *Austrochilus forsteri* Grismado, Lopardo & Platnick, 2003 and *Hickmania troglodytes* (Higgins & Petterd, 1883) by Huckstorf et al. (2015). The origin of the lateral transganglionic arteries in these species exhibit the same pattern: namely one lateral transganglionic artery that originates anteriorly in the proximal region of the pedipalpal artery, one lateral transganglionic artery that originates anteriorly in the first to fourth walking leg artery, respectively and – at the fourth walking leg artery – one lateral transganglionic artery that originates posteriorly. All lateral transganglionic arteries run between adjacent lateral neuropils. This pattern was not consistent in *A. diadematus* since the origin of the fifth lateral transganglionic arteries is subject to intraspecific variability (Fig. 4). The alternating pattern where the fifth lateral transganglionic arteries originates posteriorly from the third walking leg artery has not been described in Araneae.

The median transganglionic arteries in Araneae generally originate from five arteries connecting the right and the left aortic arches or the supraneural artery (Schneider 1892; Causard 1896; Huckstorf et al. 2013). This pattern has also been described in scorpions (Klußmann-Fricke et al. 2012, 2014), Amblypygi and Uropygi (Klußmann-Fricke & Wirkner in press). In *Araneus,* connecting arteries are missing so the origin of the median transganglionic arteries can be found at one aortic arch, the first median transganglionic artery or the supraneural artery.

Another variation found in median transganglionic arteries in different specimens (see results) points to a different rather technical problem. The injection method itself may lead to different results concerning the median transganglionic arteries due to their relative small diameters, i.e., in some specimens some of the median transganglionic arteries may have not been filled with resin. We therefore generally refrained from taking numerical variation into account in this study. All variation accounted here relates to structural differences. We therefore postulate that 12 median transganglionic arteries (the maximal number counted) occur in *A. diadematus*, but this figure is still lower than the results presented by Schneider (1892), who counted 13 median transganglionic arteries (including her "labiale post." (lp) supplying the lower lip, see below). Taking other investigations into account, it appears that the number of median transganglionic arteries varies between spider species from, for example, *Tegenaria* sp. (Schneider 1892) and *A. labyrinthica* (Causard 1896) with 13 to 12 median transganglionic arteries in *C. salei* (Huckstorf et al. 2013). The lowest number hitherto presented is for *Argyroneta aquatica* (Clerck, 1757) with six median transganglionic arteries (Crome 1952). Whether or not quantitative intraspecific variability also occurs in median transganglionic arteries still needs to be tested in a future study.

The arterial supply of the lower lip in *A. diadematus* (Fig. 3A) and in *A. quadratus* is peculiar, since the corresponding artery originates from one aortic arch and not from the cheliceral artery, as in other spiders (Causard 1896; Crome 1952; Huckstorf et al. 2013). This artery represents the elongated first median transganglionic artery (Schneider 1892). This can be deduced from its origin and its course through the subesophageal ganglion on the ventral side of the esophagus. We can therefore conclude that the lower lip artery (originating from the cheliceral artery) has been reduced in *Araneus*, while the hemolymph supply is taken over by the first median transganglionic artery.

The first median transganglionic artery and the supraneural artery can originate from the right or the left aortic arch, respectively. As illustrated in the schematic drawings (Fig. 4), all four possible combinations were present in *Araneus* (see Fig. 4). No correlation was found between the originating sides of the first median transganglionic artery and the supraneural artery.

Comparative morphology of the HVS in the opisthosoma.—*Heart:* The posterior aorta of most spiders is unbranched except for a terminal bifurcation close to the spinnerets (Fig. 1D, E) (Causard 1896; Huckstorf et al. 2013, 2015), and *A. diadematus* is no exception to this. Indeed, the only recorded account of any variation is in *Dysdera*, which displays a more anteriorly branched posterior aorta, a shortened heart and a lower number of cardiac artery systems (Schneider 1892; Causard 1896).

Ostia: Spider taxa show notable differences when comparing both the number and arrangement of ostia, and the origin of cardiac arteries. With regards to the ostia, studies by Petrunkevitch (1933) have shown how the number of pairs of ostia can vary from five (in Liphistiidae) to two. In the Mygalomorphae and Hypochilidae, the heart is equipped with four pairs of ostia. Within the Mygalomorphae, the number of ostia is reduced to three pairs in the taxa Barychelidae and Migidae. There are more independent reductions to three pairs of ostia in Filistatidae, Synspermiata and Entelegynae (see Huckstorf et al. 2015). Several taxa independently exhibit even fewer ostia – down to two pairs in taxa such as Cybaeidae, Dysderidae, Segestriidae, etc. (see Petrunkevitch 1933 for a comprehensive list). The number and position of the three ostia found in *A. diadematus* fits the ground pattern of Entelegynae and reinforces available data (Causard 1896; Willem 1917).

Cardiac artery systems: Available literature is less expansive on the subject of the cardiac arteries. However, we can find evidence of a reduction from five pairs in Liphistiidae (Millot 1933) down to two pairs in *A. aquatica* (Crome 1952) and *Segestria* sp. (Schneider 1892; Causard 1896). In Hypochilidae and Austrochilioidea the number of ostia is reduced to four, of which the posterior three are associated with a cardiac artery system (Huckstorf et al. 2015). The heart of *A. diadematus* possesses three paired ostia and three paired cardiac arteries (Fig. 2). The origin of the first and second cardiac arteries is located ventrally to the subsequent two ostia. The third cardiac artery originates in the posterior region of the heart and is not associated with a pair of ostia. This arrangement of ostia and cardiac arteries corresponds to that exhibited in Filistatidae, Synspermiata and Entelegynae (Causard 1896; Willem 1917; Huckstorf et al. 2013, 2015). The results of this study regarding the position of ostia and origin of cardiac arteries confirm the results of Causard (1896) and Willem (1917) for *A. diadematus* and contradict former descriptions of six pairs of cardiac arteries (Blanchard 1849). In comparison

the evolutionary reduction in number of ostia and of cardiac arteries show different patterns; for a detailed discussion see Huckstorf et al. (2013).

The most complex aspect of the opisthosomal HVS in spiders, the branching pattern of the cardiac artery systems, has so far been illustrated in just a few cases (Schneider 1892; Causard 1896; Crome 1952; Huckstorf et al. 2013, 2015). The only results previously available for cardiac arteries in *A. diadematus* (Blanchard 1849) have to be dismissed: the number of cardiac arteries stated makes it unreliable. The present study therefore constitutes a novel and up-to-date insight into the branching pattern of the three cardiac artery systems in *A. diadematus*.

The main artery and most of the smaller arteries of all three cardiac artery systems in *A. diadematus* run in close proximity to the cuticle to the ventral side of the body. There is only a small amount of overlap in the body regions (anterior-posterior axis) supplied by each cardiac artery system. This picture differs in *Agelena labyrinthica* where the second cardiac artery system mainly remains in the interior opisthosoma (Causard 1896). The periphery of the mid-opisthosoma is supplied by arteries extending anteriorly from the third cardiac artery system (Causard 1896). Differences can also be found in *C. salei* when comparing the regions supplied by the cardiac artery systems. In this species, the second cardiac artery system supplies the bulk of the ventral opisthosoma. Conversely, the ventral extension of the first and third cardiac artery system in the anterior and posterior part of the opisthosoma is reduced, respectively (Huckstorf et al. 2013). To date, only a few studies are available that illustrate the cardiac artery systems in detail. Therefore, the identification of morphological or phylogenetic patterns is hampered and has to be left open at this point.

Ligaments: Forming a coherent account of the ligament pattern attached to the heart within the opisthosoma in *A. diadematus* is not easy. Existing literature details differing numbers for each of the three different types of ligaments (Schimkewitsch 1884; Schneider 1892; Causard 1896; Willem 1917). The most extensive study so far on ligaments by Causard (1896) describes 11 dorsal ligaments, eight lateral ligaments and five ventral ligaments. Considering the dorsal and lateral ligaments this description differs from our findings of ten dorsal ligaments and nine lateral ligaments. However, it is obvious that there is an equal number of ligaments overall in both studies (19 dorsal and lateral ligaments). By comparing both sequences, it appears likely what we describe as the eighth lateral ligaments, was interpreted as the tenth dorsal ligaments by Causard (for further descriptions of the set of ligaments in other species see Causard 1896; Millot 1933; Crome 1952; Huckstorf et al. 2013). Because the results are too varied and are taken from an insufficient number of species, we are unable to undertake an expedient discussion here. However, further investigations on this topic are obviously needed as the ligament patterns seem to reveal information with regards to the shortening of the heart (Huckstorf et al. 2013, 2015).

Intraspecific variability.—One of the aims of our study was to highlight intraspecific variability within the HVS of *A. diadematus* by studying 33 specimens. This number far exceeds common morphological practice, in which just a few specimens are analyzed. Comparing our study with other investigations into the HVS in arthropods (Keiler et al. 2013, 2015 a, b; Huckstorf et al. 2015; Göpel & Wirkner 2015), we can conclude that there are four major patterns of intraspecific variability:

i. Variability of the course of arteries
ii. Variability of the number of off-branching arteries
iii. Variability of arterial origins
iv. Variability of the occurrence of anastomoses

Apart from the last phenomenon, all of the above-listed patterns of variability occur in the HVS of *A. diadematus*. However, in comparison to other spiders, we found that the HVS in *Araneus* differs remarkably by the tendency to reduce paired origins of arteries arranged along the body midline to an unpaired, unilateral origin. These unilateral origins are regions in which we frequently observed intraspecific variability.

Although these forms of intraspecific variability occur, there are many features and patterns that are consistent across the specimen range. These stable patterns can reliably be used for character conceptualization for phylogenetic and evolutionary analyses (Richter & Wirkner 2014).

ACKNOWLEDGMENTS

We like to thank Kerstin Schwandt for preparing histological sections and Katarina Huckstorf, Torben Göpel, Bastian-Jesper Klußmann-Fricke and Stefan Richter for fruitful discussions and technical support. Helen Johnson improved the English of this paper. Comments by Martín Ramírez and an anonymous reviewer helped to improve the manuscript further. CSW is supported by the Deutsche Forschungsgemeinschaft DFG (WI 3334/4-1).

LITERATURE CITED

Blanchard, É. 1849. De l'appareil circulatoire et des organes de la respiration dans les Arachnides. Annales des Sciences Naturelles. Zoologie 3:317–351.

Brandt, J.F. 1840. Recherches sur l'anatomie des Araignées. Annales des Sciences Naturelles 2:180–186.

Causard, M. 1896. Recherches sur l'appareil circulatoire des aranéides. Scientifique de la France et de la Belgique 29:1–109.

Claparède, É. 1863. Études sur la circulation du sang chez les aranées du genre *Lycose*. Publication de la Société de Physique et d'histoire Naturelle de Genève 17:1–22.

Crome, W. 1952. Die Respirations- und Circulationsorgane der *Argyroneta aquatica* Cl. (Araneae). Wissenschaftliche Zeitschrift der Humboldt-Universität zu Berlin 2:53–83.

Cuvier, G. 1810. Vorlesung über vergleichende Anatomie. Vierter und letzter Theil, welcher die Organe des Kreislaufs, des Athmens, der Stimme und der Generation enthält. Paul Gotthelf Kummer, Leipzig.

Gerhardt, U. & A. Kästner. 1938. Araneae. Pp. 394–656. *In* Kükenthal's Handbuch der Zoologie. (W. Kükenthal, T. Krumbach, J.-G. Helmcke, H. v. Lengerken, eds.). De Gruyter, Berlin.

Göpel, T. & C.S. Wirkner. 2015. An "ancient" complexity? Evolutionary morphology of the circulatory system in Xiphosura. Zoology 118:221–238.

Grube, E. 1842. Einige Resultate aus Untersuchungen über die Anatomie der Araneiden. Archiv für Anatomie, Physiologie und wissenschaftliche Medicin 1842:296–302.

Huckstorf, K., G. Kosok, E.–A. Seyfarth & C.S. Wirkner. 2013. The hemolymph vascular system in *Cupiennius salei* (Araneae: Ctenidae). Zoologischer Anzeiger 252:76–87.

Huckstorf, K., P. Michalik, M.J. Ramírez & C.S. Wirkner. 2015. Evolutionary morphology of the hemolymph vascular system of basal araneomorph spiders (Araneae: Araneomorphae). Arthropod Structure & Development 44:609–621.

Keiler, J., S. Richter & C.S. Wirkner. 2013. Evolutionary morphology of the hemolymph vascular system in hermit and king crabs (Crustacea: Decapoda: Anomala). Journal of Morphology 274:759–778.

Keiler, J., S. Richter & C.S. Wirkner. 2015a. The anatomy of the king crab *Hapalogaster mertensii* Brandt, 1850 (Anomura: Paguroidea: Hapalogastridae) – new insights into the evolutionary transformation of hermit crabs into king crabs. Contributions to Zoology 84:149–165.

Keiler, J., S. Richter & C.S. Wirkner. 2015b. Evolutionary morphology of the organ systems in squat lobsters and porcelain crabs (Crustacea: Decapoda: Anomala): An insight into carcinization. Journal of Morphology 276:1–21.

Klußmann-Fricke, B.–J. & C.S. Wirkner. in press. Comparative morphology of the hemolymph vascular system in Uropygi and Amblypygi (Arachnida): complex correspondences indicate monophyletic Arachnopulmonata. Journal of Morphology.

Klußmann-Fricke, B.J., S.W. Pomrehn & C.S. Wirkner. 2014. A wonderful network unraveled - Detailed description of capillaries in the prosomal ganglion of scorpions. Frontiers in Zoology 11:28.

Klußmann-Fricke, B.–J., L. Prendini & C.S. Wirkner. 2012. Evolutionary morphology of the hemolymph vascular system in scorpions: A character analysis. Arthropod Structure & Development 41:545–560.

Metscher, B.D. 2009. MicroCT for comparative morphology: simple staining methods allow high-contrast 3D imaging of diverse non-mineralized animal tissues. BMC Physiology 9:1–14.

Millot, J. 1933. Notes complémentaires sur l'anatomie des Liphistiides et des Hypochilides, a propos d'un travail récent de A. Petrunkevitch. Bulletin de la Société zoologique de France 58:217–235.

Petrunkevitch, A. 1911. Über die Circulationsorgane von *Lycosa carolinensis* Walck. Zoologische Jahrbücher, Abteilung für Anatomie 31:161–170.

Petrunkevitch, A. 1933. An inquiry into the natural classification of spiders, based on a study of their internal anatomy. Transactions of the Connecticut Acedemy of Arts and Sciences 31:299–389.

Richter, S. & C.S. Wirkner. 2014. A research program for Evolutionary Morphology. Journal of Zoological Systematics and Evolutionary Research 52:338–350.

Schimkewitsch, W. 1884. Étude sur l'anatomie de l'Épeire. Annales des Sciences Naturelles. Zoologie 17:1–94.

Schneider, A. 1892. Injections Fines. Tabelletes Zoologique 2:113–198.

Treviranus, G.R. 1812. Ueber den innern Bau der Arachniden. Johann Leonhard Schrag, Nürnberg.

Vogt, G., C.S. Wirkner & S. Richter. 2009. Symmetry variation in the heart-descending artery system of the parthenogenetic marbled crayfish. Journal of Morphology 270:221–226.

Willem, V. 1917. Observations sur la circulation sanguine et la respiration pulmonaire chez les araignées. Archives Néerlandaises de Physiologie de l'Homme et des Animaux 1:226–256.

Wirkner, C.S. 2009. The circulatory system in Malacostraca – Evaluating character evolution on the basis of differing phylogenetic hypotheses. Arthropod Systematics & Phylogeny 67:57–70.

Wirkner, C.S. & K. Huckstorf. 2013. The circulatory system of spiders. Pp. 15–27. *In* Spider Ecophysiology. (W. Nentwig, ed.). Springer-Verlag, Heidelberg.

Wirkner, C.S. & S. Richter. 2004. Improvement of microanatomical research by combining corrosion casts with microCT and 3D reconstruction, exemplified in the circulatory organs of the woodlouse. Microscopy Research and Technique 64:250–254.

Wirkner, C.S., M. Tögel & G. Pass. 2013. The arthropod circulatory system. Pp. 343–391. *In* Arthropod Biology and Evolution. Molecules, Development, Morphology. (A. Minelli, G. Boxshall, and G. Fusco, eds.). Springer-Verlag, Heidelberg.

World Spider Catalog. 2015. World Spider Catalog. Version 16.5. Natural History Museum, Bern. Online at http://www.wsc.nmbe.ch/

Manuscript received 2 January 2016, revised 5 April 2016.